World Journal of Radiology

Submit a Manuscript: http://www.wjgnet.com/esps/
Help Desk: http://www.wjgnet.com/esps/helpdesk.aspx
DOI: 10.4329/wjr.v6.i6.374

World J Radiol 2014 June 28; 6(6): 374-380
ISSN 1949-8470 (online)

CLINICAL TRIALS STUDY

Feasibility study of computed *vs* measured high b-value (1400 s/mm²) diffusion-weighted MR images of the prostate

Leonardo K Bittencourt, Ulrike I Attenberger, Daniel Lima, Ralph Strecker, Andre de Oliveira, Stefan O Schoenberg, Emerson L Gasparetto, Daniel Hausmann

Leonardo K Bittencourt, Daniel Lima, Emerson L Gasparetto, CDPI Ressonância Magnética, Avenida das Américas, 4666 Barra da Tijuca, RJ 22631-000, Brazil
Ulrike I Attenberger, Stefan O Schoenberg, Daniel Hausmann, Institute of Clinical Radiology and Nuclear Medicine, University of Heidelberg, University Hospital Mannheim, Theodor-Kutzer-Ufer 1-3, 68167 Mannheim, Germany
Ralph Strecker, Siemens Healthcare Brazil, Avenida Mutinga, 3800 Jardim Santo Elias, SP 05110-902, Brazil
Andre de Oliveira, Siemens AG Healthcare Sector, Henkestrasse 127, D-91052 Erlangen, Germany
Author contributions: Bittencourt LK and Hausmann D contributed equally to this work; Bittencourt LK, Hausmann D, Strecker R, de Oliveira A, Gasparetto EL designed the research; Hausmann D, Bittencourt LK and Strecker R performed the research; Hausmann D, Strecker R and de Oliveira A analyzed the data; Hausmann D, Bittencourt LK, Lima D, Schoenberg S, Attenberger UI and Strecker R wrote the paper.
Correspondence to: Dr. Daniel Hausmann, MD, Institute of Clinical Radiology and Nuclear Medicine, University of Heidelberg, University Hospital Mannheim, Theodor-Kutzer-Ufer 1-3, 68167 Mannheim,
Germany. daniel.hausmann@medma.uni-heidelberg.de
Telephone: +49-621-3832276 Fax: +49-621-3833817
Received: January 24, 2014 Revised: March 23, 2014
Accepted: April 17, 2014
Published online: June 28, 2014

Abstract

AIM: To evaluate the impact of computed b = 1400 s/mm² (C-b1400) *vs* measured b = 1400 s/mm² (M-b1400) diffusion-weighted images (DWI) on lesion detection rate, image quality and quality of lesion demarcation using a modern 3T-MR system based on a small-field-of-view sequence (sFOV).

METHODS: Thirty patients (PSA: 9.5 ± 8.7 ng/mL; 68 ± 12 years) referred for magnetic resonance imaging (MRI) of the prostate were enrolled in this study. All measurements were performed on a 3T MR system. For DWI, a single-shot EPI diffusion sequence (b = 0, 100, 400, 800 s/mm²) was utilized. C-b1400 was calculated voxelwise from the ADC and diffusion images. Additionally, M-b1400 was acquired for evaluation and comparison. Lesion detection rate and maximum lesion diameters were obtained and compared. Image quality and quality of lesion demarcation were rated according to a 5-point Likert-type scale. Ratios of lesion-to-bladder as well as prostate-to-bladder signal intensity (SI) were calculated to estimate the signal-to-noise-ratio (SNR).

RESULTS: Twenty-four lesions were detected on M-b1400 images and compared to C-b1400 images. C-b1400 detected three additional cancer suspicious lesions. Overall image quality was rated significantly better and SI ratios were significantly higher on C-b1400 (2.3 ± 0.8 *vs* 3.1 ± 1.0, $P < 0.001$; 5.6 ± 1.8 *vs* 2.8 ± 0.9, $P < 0.001$). Comparison of lesion size showed no significant differences between C- and M-b1400 ($P = 0.22$).

CONCLUSION: Combination of a high b-value extrapolation and sFOV may contribute to increase diagnostic accuracy of DWI without an increase of acquisition time, which may be useful to guide targeted prostate biopsies and to improve quality of multiparametric MRI (mMRI) especially under economical aspects in a private practice setting.

Key words: Prostate cancer; Magnetic resonance imaging; Diffusion-weighted imaging; Ultra-high b-values; Extrapolated b-values

Core tip: Prostate cancer is the most common malignant tumor entity in males. Combination of a high b-value extrapolation and small-field-of-view sequence readout may contribute to increase diagnostic accuracy

of diffusion-weighted images without an increase of acquisition time, which may be useful to guide targeted prostate biopsies and to improve quality of multiparametric magnetic resonance imaging especially under economical aspects in a private practice setting.

Bittencourt LK, Attenberger UI, Lima D, Strecker R, de Oliveira A, Schoenberg SO, Gasparetto EL, Hausmann D. Feasibility study of computed *vs* measured high b-value (1400 s/mm²) diffusion-weighted MR images of the prostate. *World J Radiol* 2014; 6(6): 374-380 Available from: URL: http://www.wjgnet.com/1949-8470/full/v6/i6/374.htm DOI: http://dx.doi.org/10.4329/wjr.v6.i6.374

INTRODUCTION

Prostate cancer (PCa) is currently the most commonly diagnosed non-skin cancer and the second leading cause of cancer related death in the United States[1]. Recent technical improvements such as the beneficiary SNR gains of higher field strength made MRI a valuable diagnostic measure that allows to detect prostate cancer with a high diagnostic accuracy even at earlier disease stages[2]. Multi-parametric MR (mMRI) imaging is the mainstay of prostate cancer imaging[3-6], most commonly consisting of T2-weighted imaging (T2w), diffusion-weighted-imaging (DWI), dynamic contrast-enhanced imaging (DCE) and proton MR spectroscopy imaging (MRSI)[7-10]. Among those, DWI is probably the most promising technique, especially for detection of peripheral zone (pz) tumors and estimation of Pca aggressiveness[11-13], but also for monitoring therapy[14]. Recent studies indicate that the measurement of high b-values (2000 s/mm^2) increases the lesion detection rate[15], even though the ability to discriminate malignant from benign tissue in the pz is limited due to a significant overlap of ADC-values[16]. In clinical routine, the standard protocol commonly involves b-values from 0 to 800 s/mm^2. The use of higher b-values is currently limited by the two following factors: reduction of SNR at b-values > 1000 s/mm^2 due to T2 signal decay as a consequence of a prolonged TE[17] and cost effectiveness considerations due to a prolonged acquisition time, especially in a private practice setting. Due to these shortcomings, techniques that allow for the calculation of a high b-value DWI based on routinely measured lower b-values[18] seem to be appealing. In this context, recent studies indicate that computed DWI (cDWI) is feasible with good SNR and without additional scan time, which may improve disease detection[18].

On the one hand high field strength imaging at 3 Tesla (T) with higher intrinsic SNR is superior to 1.5 T for the detection of prostate cancer[19], on the other hand susceptibility artifacts related to the proximity of the pz to the air-filled rectum are more relevant. Recently, small FOV (sFOV) imaging strategies for DWI based on[20] the use of 2d radiofrequency (RF) excitation pulses for the excitation of a small volume spanning of the prostate region only were developed to overcome these shortcomings of 3T MRI[21] and allow for a reduction of artifacts and a smooth fusion with morphologic T2w images. For this study a b1400 sequence was extrapolated from a sFOV and low (< 1000 s/mm^2) b-value protocol to combine the advantages of reduced distortion artifacts and higher SNR of computed images. The purpose of this study is to compare lesion detection rate, image quality and quality of lesion demarcation of a computed (C-b1400) and a measured b = 1400 s/mm^2 (M-b1400) sequence based on a sFOV image set utilizing a modern 3T MR-system.

MATERIALS AND METHODS

Study population

Thirty consecutive patients (median PSA: 9.5 ± 8.7 ng/mL; mean age: 68 ± 12 years) who underwent functional prostate MR at our institution were enrolled in this study.

Among the indications for the study, 21 patients were referred due to elevated PSA levels, 4 for PCa staging, 4 for surveillance of post-treatment recurrence and one for suspected prostatitis.

MR Imaging

All measurements were performed on a 3 T clinical whole-body MR scanner (Verio, Siemens Healthcare, Erlangen, Germany) and state-of-the-art mMRI parameters were applied[19]. One hundred mL endorectal gel was administered prior to the examination, in order to reduce artifacts due to heterogeneous rectal content. For DWI, a single-shot EPI diffusion sequence with the following parameters was utilized: TE/TR= 63/4200 ms, 8 averages, FOV 300 mm × 93 mm, matrix 192 × 60, slice thickness 3.6 mm, no gap, SPAIR fat saturation, b-values = 0, 100, 400, 800 s/mm². An outer volume suppression by two sharp defined coronal saturation bands was applied which allowed to reduce the acquisition to a small rectangular FOV with an inplane resolution of 1.5 mm × 1.5 mm to gain SNR and to reduce distortion artifcats. The conventional full excitation was used in the sequence, followed by a short EPI readout covering only the sFOV in anterior-posterior direction. Total scan time for this sequence was 5 min 49 s. The ADC was calculated from diffusion images with all the measured b-values. C-b1400 was calculated voxelwise from the ADC and diffusion images according to:

$S(b_{1400}) = S0 * \exp(- ADC*b_{1400})$ with the pixel intensity SO in b = 0 s/mm².

A b-value of 1400 s/mm² was chosen to keep sequence parameters similar. Additionally, the M-b1400 sequence (b = 1400 s/mm², TE/TR = 73/4400 ms, all other parameters identical, duration: 1min45s) was acquired immediately after the original DWI sequence for evaluation and comparison (Figure 1).

Image analysis

Data sets of every patient were analyzed by two radiologists (DH, 3 years of experience in prostate imaging) and (LKB, 6 years of experience in prostate imaging) in con-

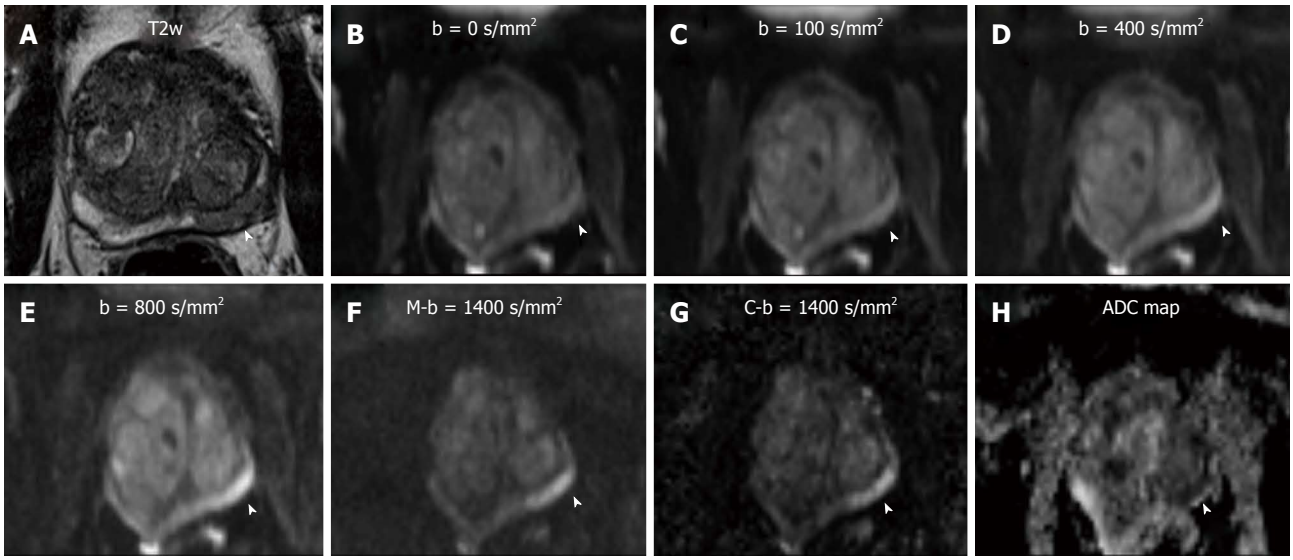

Figure 1 Axial T2-weighted image of an 88 years old patient with a PSA level of 8.2 ng/mL and negative findings upon digital rectal examination. T2w shows a focal hypointense lesion in the posterolateral left midgland pz (arrowhead in A). Measured b-values of 0, 100, 400 and 800 s/mm² (arrowheads in B, C, D and E, respectively) do not depict the suspected lesion with sufficient contrast to background prostate. M-b1400 shows good lesion-to-prostate contrast (arrowhead in F). C-b1400 depicts the lesion with the same lesion-to-prostate contrast and a slightly improved demarcation (arrowhead in G). The ADC value of the suspicious lesion was as low as 648 × 10^{-3} mm/s² [ADC map (H)].

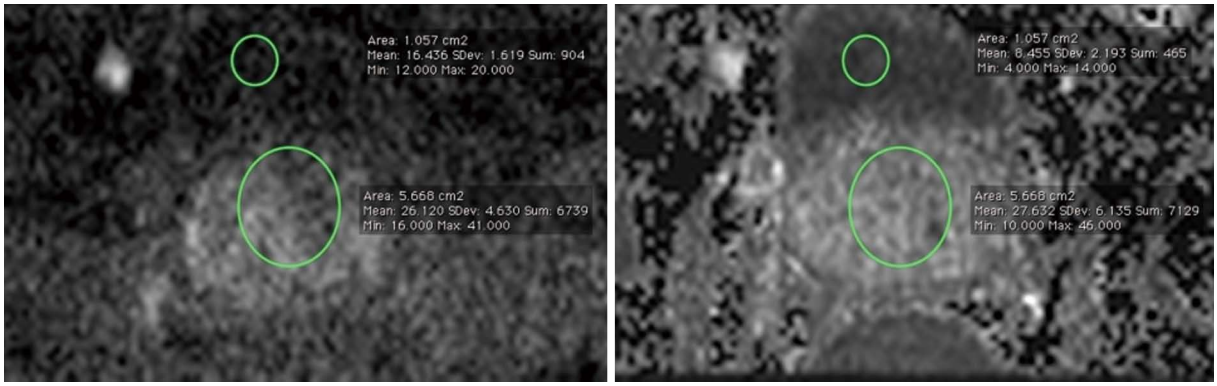

Figure 2 M-b1400 (left) and C-b1400 (right) images of a 63 years old patient with elevated PSA levels, at corresponding axial slice position. Region-of-interests were placed in the prostate and in the bladder content to obtain signal intensity-ratios to estimate signal-to-noise-ratio. Calculated b-value images show higher SI-ratios and more anatomical image details (*i.e.*, bladder contour).

sensus, For the measurement of prostate signal intensity, a region-of-interest (ROI) was placed overlying the visualized portion of the prostate at the level of the bladder. Another ROI which was placed in the bladder content served as reference. The size and the localization of these ROIs were chosen identical on both the C-b1400 and M-b1400, to allow for an adequate comparison (Figure 2).

Lesion detection rate (cancer suspicious lesions) as well as lesion diameters were obtained and compared. Image quality, quality of lesion demarcation and diagnostic confidence of the observers were rated according to a 5-point Likert-type scale from "1" ("excellent") to "5" ("poor"). Lesion-to-bladder and prostate-to-bladder signal-intensity (SI) ratios were obtained and compared to estimate signal-to-noise-ratio (SNR).

Statistical analysis

SPSS (Version 20; IBM SPSS Statistics, United States) was used for statistical analysis. Measured values did not show Gaussian distribution so Wilcoxon-tests were performed for comparison of C-b1400 and M-b1400.

RESULTS

Patients and lesions

In 30 consecutive patients, a total of 27 lesions were evaluated. Lesions were rated as prostate cancer (n = 15), nodules of benign prostate hyperplasia (BPH) (n = 8) and cancer recurrence (n = 4). Two patients presented with locally recurrent cancer after prostatectomy.

Image quality, lesion detection rate, lesion demarcation and diagnostic confidence

Image quality was rated significantly better in C-b1400 (mean = 2.3 ± 0.8) compared to M-b1400 (mean = 3.1 ± 1.0; P < 0.001). Moreover, the computed images sub-

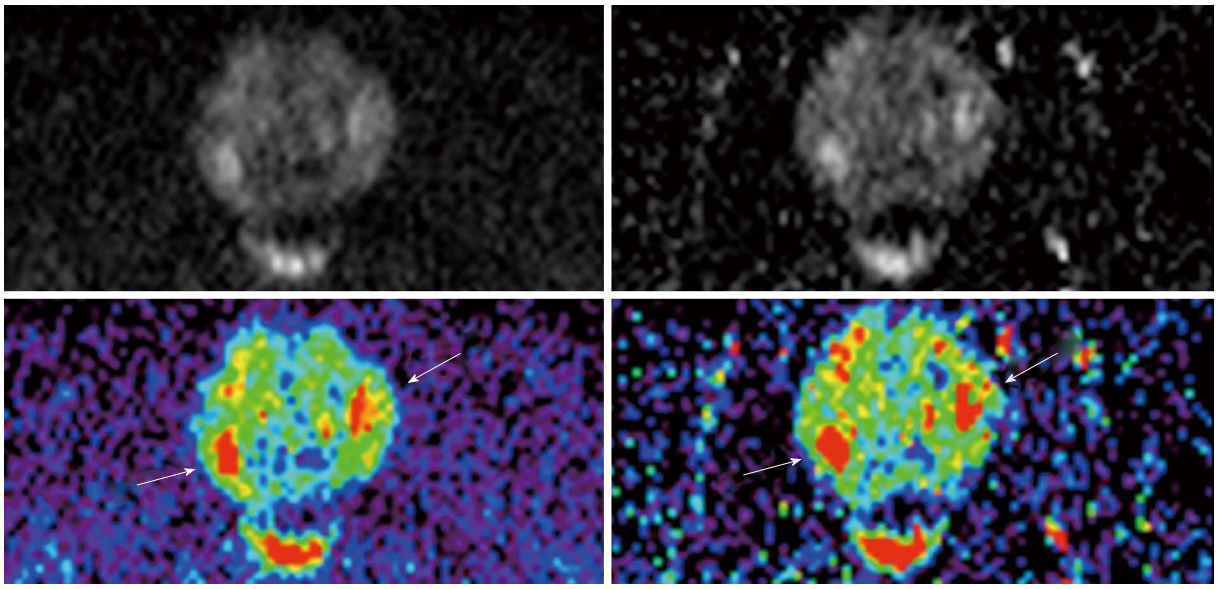

Figure 3 M-b1400 (left column) and C-b1400 (right column) images of the same patient. Demarcation of two oval hyperintense suspicious lesions is very good on both images (arrows).

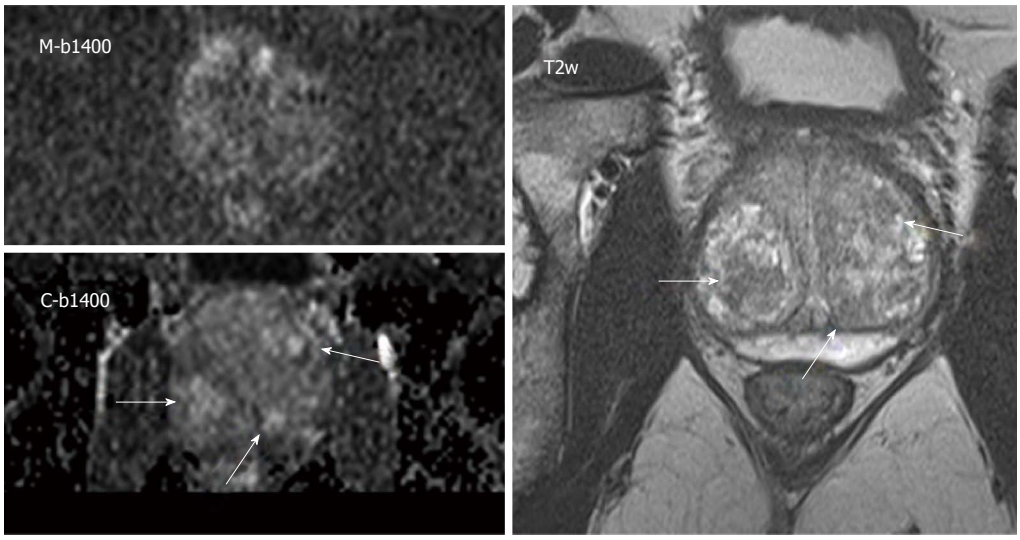

Figure 4 Images of a 68 years old patient with elevated PSA levels and signs of benign prostate hyperplasia. M-b1400 (upper image on the left) was acquired with reduced image quality due to distortion artifacts. The C-b1400 (below) in corresponding slice position and identical window level shows an improved image quality with demarcation of several lesions that were rated as benign benign prostate hyperplasia-nodules taking into account T2w (right image) and dynamic contrast-enhanced imaging.

jectively showed more anatomical detail. We did not find significant differences regarding the quality of lesion demarcation with a trend to better results of C-b1400 (mean = 2.6 ± 1.0 *vs* 2.8 ± 0.9, respectively; $P = 0.29$) (Figures 3 and 4).

C-b1400 detected 3 additional cancer suspicious lesions compared to M-b1400 images, which were confirmed by ADC maps, T2w and DCE evaluation. Overall diagnostic confidence was rated slightly better on C-b1400, even though results were not significantly different (2.2 ± 0.9 *vs* 2.1 ± 0.8, $P = 0.48$, respectively) (Table 1).

SI-ratios and lesion size

Significantly higher SI-ratio of prostate-to-bladder and lesion-to-bladder were obtained for C-b1400 compared to M-b1400 ($P < 0.001$ and $P < 0.001$, respectively).

Comparison of lesion size showed no significant differences between calculated and measured images ($P < 0.22$) (Table 2). All statistical data are given as means and standard deviations.

DISCUSSION

The study compared lesion detection rate, image quality and quality of lesion demarcation of a C-b1400 derived from a standard DWI protocol with M-b1400 images. A significantly better image quality of the C-b1400 was observed. Moreover, C-b1400 revealed more additional sus-

Table 1 Comparison of C-b1400 and M-b1400 images; image qualitiy, quality of lesion demarcation and level of confidence were rated according to a 5-point Likert-type scale

b = 1400 s/mm^2	Image quality (n = 30)	Lesion demarcation (n = 24)	Diagnostic confidence (n = 30)
M-b1400	3.1 ± 1.0	2.8 ± 0.9	2.2 ± 0.9
C-b1400	2.3 ± 0.8	2.6 ± 1.0	2.1 ± 0.8
P-value	< 0.001	0.29	0.48

Table 2 Objective parameters: Prostate-to-bladder and lesion-to-bladder signal intensity ratios were obtained to estimate signal-to-noise-ratio and contrast-to-noise ratio

b = 1400 s/mm^2	SI prostate/bladder (n = 28)	SI lesion/bladder (n = 24)	Lesion diameter (mm) (n = 24)
M-b1400	1.9 ± 0.5	2.8 ± 0.9	16.9 ± 10.0
C-b1400	3.7 ± 1.0	5.6 ± 1.8	17.7 ± 10.0
P-value	< 0.001	< 0.001	0.22

Lesion diameters are presented in units of mm. SI: Signal intensity.

picious lesions that were confirmed by comparison with ADC maps and T2w. C-b1400 exhibited higher prostate-to-bladder and lesion-to-bladder SI ratios than M-b1400, which could indicate better SNR.

Multiple studies have tried to determine an optimal b-value to visualize prostate cancer using DWI at 3 T. A study by Metens *et al*[22] assessed examinations of forty-one patients with biopsy proven prostate cancer who underwent 3 T DWI performed with 5 b-values (1000, 1500, 2000 and 2500 s/mm^2) using a 16-channel coil. Best lesion visibility, the central gland-to-lesion (CG-L) and the peripheral zone-to-lesion (PZ-L) contrast-to-noise ratio (CNR) were compared between different b-value images. In a subset of 29 patients a high resolution b = 1500 s/mm^2 DWI sequence was additionally assessed. The b = 1500 s/mm^2 and b = 2000 s/mm^2 images provided the best lesion visibility. The highest CG-L and PZ-L CNR were obtained with b = 1500 s/mm^2 ($P < 0.01$).

Another recent study assessed the diagnostic accuracy of 3T DWI for detection of prostate cancer by using different b-values. Seventy-three patients underwent MRI at 3 T. Three MRI sets were reviewed by two radiologists: MRI and DWI (b = 500 s/mm^2) (protocol A), MRI and DWI (b = 1000 s/mm^2) (protocol B), and MRI and DWI (b = 2000 s/mm^2) (protocol C). Areas under the receiver operating characteristic curve (AUCs) were calculated. The mean of the AUCs in protocol C was larger than those in protocol A and in protocol B ($P < 0.05$). The authors concluded that a b-value = 2000 s/mm^2 at 3 T can improve the diagnostic accuracy for detection of prostate cancer[15]. On the other hand, a study to determine whether the ADC obtained from a high b-value (2000 s/mm^2) is superior to that obtained from a standard b-value (1000 s/mm^2) in a monoexponential model to discriminate malignant from benign pz tissue found little diagnostic advantage of the high b-value due to significant ADC overlap[16].

Blackledge *et al*[18] described a method to extrapolate high-b-value images from DWI performed at lower b-values which allowed for an improved lesion conspicuity. Computation of DWI resulted in a higher SNR compared with measured DWI, especially at b-values > 840 s/mm^2. Moreover, in oncologic patients, a computed b-value of 2000 s/mm^2 showed good image quality and high background suppression. Evaluation of images with a computed b-value of 2000 s/mm^2 resulted in higher overall diagnostic sensitivity (96.0%) and specificity (96.6%), compared with a measured b-value of 900 s/mm^2 (sensitivity, 89.4%; specificity, 87.5%; $P < 0.01$).

In concordance with this study, our results suggest that computed b1400-images can be obtained with a better image quality due to lesser artifacts and more anatomical detail than measured b1400-images, probably as a benefit of the high SNR of the original lower b-value image sets. Nevertheless, there was no significant difference of the overall diagnostic confidence between the two image sets with a trend to better results for C-b1400 indicating a similar diagnostic performance of both, even though objectively three additional cancer suspicious lesions could be detected on C-b1400. Moreover, the comparison of the diameters of the largest lesions on measured and computed b1400 images did not reveal a significant difference between the techniques (Table 2).

Our study had a number of limitations. First of all, due to the private practice setting, there was no histopathologic confirmation of the assigned lesions. Then again, the study predominantly focused on image quality, lesion detection rate and lesion conspicuity. With regards to the reported ADC overlap of lesions, we believe that the primary value of the presented technique is to detect and draw attention to any lesion. The dignity of these lesions should be evaluated taking into account the clinical context of the patients and additional sequences such as T2w, DCE and MRSI. Moreover, we applied a mono-exponential model for the computation of C-b1400 images. Several recent publications report that there is a significant deviation from a pure Gaussian probabilistic model when applying high b-values ⩾ 1000 s/mm^2. It was confirmed that the deviation quantified by kurtosis has a greater sensitivity than ADC or the diffusion constant D for the differentiation between PCa and benign lesions of the pz (93.3% *vs* 78.5% and 83.5%)[23]. A more recently published study shows that kurtosis has the best performance in differentiating PCa from benign prostate, using different sets of b-values[24]. In both studies, high b-values up to 2000-2300 s/mm^2 were applied for acquisition which results in a relevant deviation from a pure Gaussian probabilistic model. On the other hand, the impact of kurtosis in ADC calculation using lower b-values up to 800 is small and can be neglected, which falls in the range of the b-values acquired in the present study[25]. Furthermore, in this preliminary feasibility study, patients were included consecutively, and the indications and clinical contexts for the examinations were not homogeneous. In addition, a major concern of b-values above 1000 s/mm^2 in DWI aquisition is their intrinsically lower SNR

and the consecutive compromise of the calculation of the ADC. In clinical practice, stronger diffusion encodings are usually achieved by the prolongation of the motion probing gradients, which leads to a longer TE and an increased T2 decay of the signal. As a result, the highest chosen b-value ultimately determines the TE of the whole diffusion scan and may thus affect the SNR of the whole image set. It is therefore appealing to avoid signal loss by maintaing a shorter TE for conventional diffusion acqusition protocol, while associating the computation of high b-value image sets (*i.e.*, above b = 1200 s/mm^2), in order to benefit from the better SNR of the calculated ADC. In this study, only the readout was reduced to a sFOV, whereas more sophisticated techniques combine a sFOV readout with a sFOV excitation pulse[20]. Finally, a direct measurement of SNR was not feasible due to the sFOV which did not allow for inclusion of surrounding air for precise calculations. Nevertheless, the prostate-to-bladder and lesion-to-bladder SI ratios were calculated as a potential surrogate for the actual SNR.

In conclusion, computed high b-value images derived from a sFOV DWI protocol is clinically feasible and may increase accuracy in comparison to measured b = 1400 s/mm^2 images, without an increase of examination time, which is especially important regarding further application in clinical routine in a time and cost-efficient manner. Additionally, this approach allows for the calculation of virtually any given b-value from the originally measured DWI sequence, which can be further fine-tuned for different clinical settings and applications.

Combination of a high b-value extrapolation and sFOV readout may contribute to increase diagnostic accuracy of DWI without an increase of acquisition time, which may be useful to guide targeted prostate biopsies and to improve quality of mMRI especially under economical aspects in a private practice setting. However, further studies are needed to proof the preliminary results of this study in larger cohorts of clinical patients.

COMMENTS

COMMENTS

Prostate cancer is the most common malignant tumor entity in males. Differentiation between benign and malignant prostatic disease is hindered by a similar appearance on morphologic images. Multiparametric magnetic resonance imaging (mMRI), mostly consisting of high-resolution T2-weighted sequences, Dynamic Contrast Enhanced Imaging (DCE) and Diffusion-Weighted Imaging (DWI) has extensively improved sensitivity and specificity of the examination. It has been demonstrated that high b-values of DWI contribute to improve lesion detection rate which helps to guide targeted prostate biopsies. These high b-values can either be measured directly or extrapolated based on a standard low b-value DWI sequence.

Research frontiers

The use of higher b-values is currently limited by the two following factors: reduction of SNR at b-values > 1000 s/mm^2 due to T2 signal decay as a consequence of a prolonged TE and cost effectiveness considerations due to a prolonged acquisition time, especially in a private practice setting. Due to these shortcomings, techniques that allow for the calculation of a high b-value DWI based on routinely measured lower b-values seem to be appealing. On the one hand high field strength imaging at 3 Tesla with higher intrinsic SNR is superior to 1.5 T for the detection of prostate cancer, on the other hand susceptibility artifacts related to the proximity of the peripheral zone to the air-filled rectum are more relevant. Recently, small FOV (sFOV) imaging strategies for DWI based on the use of 2d radiofrequency excitation pulses for the excitation of a small volume spanning of the prostate region only were developed to overcome these shortcomings of 3T MRI and allow for a reduction of artifacts and a smooth fusion with morphologic T2w images

Innovations and breakthroughs

For this study a b1400 sequence was extrapolated from a sFOV and low (< 1000 s/mm^2) b-value protocol to combine the advantages of reduced distortion artifacts and higher SNR of computed images. The purpose of this study is to compare lesion detection rate, image quality and quality of lesion demarcation of a computed (C-b1400) and a measured b = 1400 s/mm^2 (M-b1400) sequence based on a sFOV image set utilizing a modern 3T MR-system.

Applications

The study results suggest that extrapolated high b-value images may contribute to increase lesions detection rate in a cost- and time efficient manner, which may help to guide targeted prostate biopsies.

Terminology

Prostate cancer: Early prostate cancer usually causes no symptoms. Sometimes, however, prostate cancer does cause symptoms, often similar to those of diseases such as benign prostatic hyperplasia; Diffusion-weighted Imaging (DWI): DWI measures the movement of protons in between cells and is related to cell density. Low b-value images are rather T2-weighted and are sensitive to "T2-shine-through"-effects whereas high b-values are more useful to evaluate the properties of tissue diffusability.

Peer review

The authors compared the utility of computed *vs* measured high b-value DWI for the assessment of prostate lesions. It is well written.

REFERENCES

1 **Brawley OW**. Prostate cancer epidemiology in the United States. *World J Urol* 2012; **30**: 195-200 [PMID: 22476558 DOI: 10.1007/s00345-012-0824-2]

2 **Klimberg I**, Locke DR, Madore RA, Smith WW. Early prostate cancer: is there a need for new treatment options? *Urol Oncol* 2003; **21**: 105-116 [PMID: 12856638 DOI: 10.1016/S1078-1439(02)00211-9]

3 **Weidner AM**, Michaely HJ, Lemke A, Breitinger L, Wenz F, Marx A, Schoenberg SO, Dinter DJ. Value of multiparametric prostate MRI of the peripheral zone. *Z Med Phys* 2011; **21**: 198-205 [PMID: 21247742 DOI: 10.1016/j.zemedi.2010.12.004]

4 **Turkbey B**, Pinto PA, Mani H, Bernardo M, Pang Y, McKinney YL, Khurana K, Ravizzini GC, Albert PS, Merino MJ, Choyke PL. Prostate cancer: value of multiparametric MR imaging at 3 T for detection--histopathologic correlation. *Radiology* 2010; **255**: 89-99 [PMID: 20308447 DOI: 10.1148/radiol.09090475]

5 **Caldas ME**, Miranda LC, Bittencourt LK. Magnetic resonance imaging in staging of locoregional prostate cancer: comparison of results with analysis post-surgical histopathology. *Rev Col Bras Cir* 2010; **37**: 447-449 [PMID: 21340261]

6 **Hoeks CM**, Barentsz JO, Hambrock T, Yakar D, Somford DM, Heijmink SW, Scheenen TW, Vos PC, Huisman H, van Oort IM, Witjes JA, Heerschap A, Fütterer JJ. Prostate cancer: multiparametric MR imaging for detection, localization, and staging. *Radiology* 2011; **261**: 46-66 [PMID: 21931141 DOI: 10.1148/radiol.11091822]

7 **Scheenen TW**, Fütterer J, Weiland E, van Hecke P, Lemort M, Zechmann C, Schlemmer HP, Broome D, Villeirs G, Lu J, Barentsz J, Roell S, Heerschap A. Discriminating cancer from noncancer tissue in the prostate by 3-dimensional proton magnetic resonance spectroscopic imaging: a prospective multicenter validation study. *Invest Radiol* 2011; **46**: 25-33 [PMID: 21188832 DOI: 10.1097/RLI.0b013e3181f54081]

8 **Scherr MK**, Seitz M, Müller-Lisse UG, Ingrisch M, Reiser MF, Müller-Lisse UL. MR-perfusion (MRP) and diffusion-weighted imaging (DWI) in prostate cancer: quantitative and model-based gadobenate dimeglumine MRP parameters in detection of prostate cancer. *Eur J Radiol* 2010; **76**: 359-366

[PMID: 20471189 DOI: 10.1016/j.ejrad.2010.04.023]
9 **Schlemmer HP**. [Multiparametric MRI of the prostate: method for early detection of prostate cancer?]. *Rofo* 2010; **182**: 1067-1075 [PMID: 20972932 DOI: 10.1055/s-0029-1245786]
10 **Fütterer JJ**, Heijmink SW, Scheenen TW, Veltman J, Huisman HJ, Vos P, Hulsbergen-Van de Kaa CA, Witjes JA, Krabbe PF, Heerschap A, Barentsz JO. Prostate cancer localization with dynamic contrast-enhanced MR imaging and proton MR spectroscopic imaging. *Radiology* 2006; **241**: 449-458 [PMID: 16966484 DOI: 10.1148/radiol.2412051866]
11 **Bittencourt LK**, Barentsz JO, de Miranda LC, Gasparetto EL. Prostate MRI: diffusion-weighted imaging at 1.5T correlates better with prostatectomy Gleason Grades than TRUS-guided biopsies in peripheral zone tumours. *Eur Radiol* 2012; **22**: 468-475 [PMID: 21913058 DOI: 10.1007/s00330-011-2269-1]
12 **Oto A**, Yang C, Kayhan A, Tretiakova M, Antic T, Schmid-Tannwald C, Eggener S, Karczmar GS, Stadler WM. Diffusion-weighted and dynamic contrast-enhanced MRI of prostate cancer: correlation of quantitative MR parameters with Gleason score and tumor angiogenesis. *AJR Am J Roentgenol* 2011; **197**: 1382-1390 [PMID: 22109293 DOI: 10.2214/AJR.11.6861]
13 **Somford DM**, Hambrock T, Hulsbergen-van de Kaa CA, Fütterer JJ, van Oort IM, van Basten JP, Karthaus HF, Witjes JA, Barentsz JO. Initial experience with identifying high-grade prostate cancer using diffusion-weighted MR imaging (DWI) in patients with a Gleason score ≤ 3 + 3 = 6 upon schematic TRUS-guided biopsy: a radical prostatectomy correlated series. *Invest Radiol* 2012; **47**: 153-158 [PMID: 22293513]
14 **Park SY**, Kim CK, Park BK, Park W, Park HC, Han DH, Kim B. Early changes in apparent diffusion coefficient from diffusion-weighted MR imaging during radiotherapy for prostate cancer. *Int J Radiat Oncol Biol Phys* 2012; **83**: 749-755 [PMID: 22154286]
15 **Ohgiya Y**, Suyama J, Seino N, Hashizume T, Kawahara M, Sai S, Saiki M, Munechika J, Hirose M, Gokan T. Diagnostic accuracy of ultra-high-b-value 3.0-T diffusion-weighted MR imaging for detection of prostate cancer. *Clin Imaging* 2012; **36**: 526-531 [PMID: 22920357 DOI: 10.1016/j.clinimag.2011.11.016]
16 **Kitajima K**, Kaji Y, Kuroda K, Sugimura K. High b-value diffusion-weighted imaging in normal and malignant peripheral zone tissue of the prostate: effect of signal-to-noise ratio. *Magn Reson Med Sci* 2008; **7**: 93-99 [PMID: 18603841 DOI: 10.2463/mrms.7.93]
17 **Dietrich O**, Biffar A, Baur-Melnyk A, Reiser MF. Technical aspects of MR diffusion imaging of the body. *Eur J Radiol* 2010; **76**: 314-322 [PMID: 20299172 DOI: 10.1016/j.ejrad.2010.02.018]
18 **Blackledge MD**, Leach MO, Collins DJ, Koh DM. Computed diffusion-weighted MR imaging may improve tumor detection. *Radiology* 2011; **261**: 573-581 [PMID: 21852566 DOI: 10.1148/radiol.11101919]
19 **Barentsz JO**, Richenberg J, Clements R, Choyke P, Verma S, Villeirs G, Rouviere O, Logager V, Fütterer JJ. ESUR prostate MR guidelines 2012. *Eur Radiol* 2012; **22**: 746-757 [PMID: 22322308]
20 **Reischauer C**, Wilm BJ, Froehlich JM, Gutzeit A, Prikler L, Gablinger R, Boesiger P, Wentz KU. High-resolution diffusion tensor imaging of prostate cancer using a reduced FOV technique. *Eur J Radiol* 2011; **80**: e34-e41 [PMID: 20638208 DOI: 10.1016/j.ejrad.2010.06.038]
21 **Finsterbusch J**. Improving the performance of diffusion-weighted inner field-of-view echo-planar imaging based on 2D-selective radiofrequency excitations by tilting the excitation plane. *J Magn Reson Imaging* 2012; **35**: 984-992 [PMID: 22170770]
22 **Metens T**, Miranda D, Absil J, Matos C. What is the optimal b value in diffusion-weighted MR imaging to depict prostate cancer at 3T? *Eur Radiol* 2012; **22**: 703-709 [PMID: 21971824 DOI: 10.1007/s00330-011-2298-9]
23 **Rosenkrantz AB**, Sigmund EE, Johnson G, Babb JS, Mussi TC, Melamed J, Taneja SS, Lee VS, Jensen JH. Prostate cancer: feasibility and preliminary experience of a diffusional kurtosis model for detection and assessment of aggressiveness of peripheral zone cancer. *Radiology* 2012; **264**: 126-135 [PMID: 22550312 DOI: 10.1148/radiol.12112290]
24 **Mazzoni LN**, Lucarini S, Chiti S, Busoni S, Gori C, Menchi I. Diffusion-weighted signal models in healthy and cancerous peripheral prostate tissues: comparison of outcomes obtained at different b-values. *J Magn Reson Imaging* 2014; **39**: 512-518 [PMID: 23723087]
25 **Quentin M**, Blondin D, Klasen J, Lanzman RS, Miese FR, Arsov C, Albers P, Antoch G, Wittsack HJ. Comparison of different mathematical models of diffusion-weighted prostate MR imaging. *Magn Reson Imaging* 2012; **30**: 1468-1474 [PMID: 22819178]

P- Reviewers: Desai DJ, Msaouel P **S- Editor**: Wen LL
L- Editor: A **E- Editor**: Zhang DN

Published by **Baishideng Publishing Group Inc**
8226 Regency Drive, Pleasanton, CA 94588, USA
Telephone: +1-925-223-8242
Fax: +1-925-223-8243
E-mail: bpgoffice@wjgnet.com
Help Desk: http://www.wjgnet.com/esps/helpdesk.aspx
http://www.wjgnet.com